AD-A079 754 NAVAL OCEAN RESEARCH AND DEVELOPMENT ACTIVITY NSTL S--ETC F/G 17/9
AN EVALUATION OF ERIM X-L BAND AIRBORNE SYNTHETIC APERTURE RADA--ETC(U)
JUL 78 R D KETCHUM

UNCLASSIFIED NORDA-TN-28 NL

1 OF 1
AD-
A079754

END
DATE
FILMED
2-80
DDC

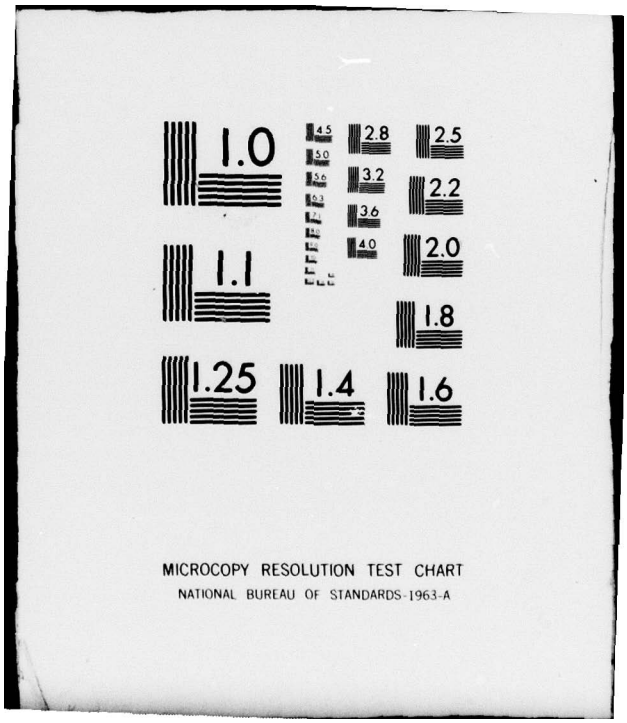

[redacted]

[redacted]

[redacted]

[redacted]

FOREWORD

The evaluation and use of various airborne remote sensor data for the study of sea ice conditions in differing sea ice regimes is a continuting task of the NORDA Polar Oceanography Branch. In addition to providing information for sea ice investigations, these evaluations provide a better understanding and background for the use of similar remote sensor data from satellite platforms which make large scale temporal and spatial studies more feasible. The ERIM X-L band synthetic aperture radar (SAR) imagery collected in this investigation to characterize the sea ice in the Labrador Sea represents a step forward in this respect because the L-band radar simulates planned SEASAT-A SAR parameters. With increasing improvements in satellite-borne active and passive microwave system capabilities, these sensors will ultimately become the primary sensors for large scale ice dynamic studies because they are independent of light and weather conditions.

ABSTRACT

Results of an evaluation of the ERIM X-L band airborne synthetic aperture radar imagery of sea ice in the Labrador Sea are given. Incident sea and swell and surface winds in this area produce complex and chaotic ice conditions with very rough surfaced ice breccias being the dominant form. It was possible to extract more information concerning the ice conditions when using both radar frequencies and polarizations. Surface roughness differences and distribution were more accurately determined using the X-band radar imagery. Variations in the nature of the surface roughness are sometimes evident due to their varying polarizing effect on the X-band radar. Floe distribution is better displayed by the L-band radar imagery, but only minor differences were recorded by the two L-band radar polarizations. The analysis shows that the X-band radar is more sensitive to ice surface properties, but that surface penetration and subsurface interfaces may account for much of the L-band radar backscatter. There are some indications of X-band radar subsurface return and depolarization in some very early stages of ice development. This suggests that sea ice crystal structure, size, and orientation in these early stages of ice development may be important contributors to the backscatter and polarization effects on radar energy which has penetrated the surface.

CONTENTS

ILLUSTRATIONS

AN EVALUATION OF ERIM X-L BAND AIRBORNE SYNTHETIC APERTURE RADAR IMAGERY OF SEA ICE

I. INTRODUCTION

This report describes an evaluation of sea ice imagery obtained during Project SAR 77, a program funded by the Canadian Government with assistance from the Office of Naval Research. The purpose of the program was to investigate the characterization of X- and L-band airborne synthetic aperture radar (SAR) imagery of sea ice. The radar data were collected by the Environmental Research Institute of Michigan (ERIM) under the auspices of the Canadian Center for Cold Ocean Resources Engineering (C-CORE), Memorial University of Newfoundland.

All of the sea ice radar imagery has been gleaned, but only that area in the Labrador Sea off Hopedale Run which was imaged on 13 March 1977 has been considered here because acceptable photography was obtained simultaneously with the SAR data on that date, making interpretive evaluation more practical. Much of the photography was not useful for accurate interpretation because of the high oblique angle and often great distances to the sea ice features.

II. SEA ICE CONDITIONS

Sea ice conditions in the Labrador Sea are very chaotic and complex. Moving southward at a relatively rapid rate, the ice fields in the Labrador Sea are continually subjected to changes in wind speed and direction and incident sea and swell, all of which join to produce a diverse conglomerate of broken ice forms and features. The ice here is derived from three sources: (1) Drift ice which formed in Baffin Bay or Davis Strait and moved southward into the area; (2) locally formed fast ice which formed in the bays and inlets and outward a short distance into the Labrador Sea (fragments of this ice have been broken away and included with the drifting ice); and (3) drift ice which formed in the Labrador Sea. All these sources have experienced the effects of wind, sea, and swell which have caused significant interactions within the ice fields producing a complex mixture of deformed ice cakes and small floes, often frozen together, in a matrix of brash and other small forms. The ice breccias, formed by the freezing together of the many small floes of different ages and thickness (most in the first-year ice categories), are the primary ice form in this area. They are generally weak and may possess a wide range of morphological and physical properties over relatively small areas. The secondary ice cover is provided by the unconsolidated, usually close to very close packed matrix of brash and other small broken forms between the floes. This ice condition becomes the dominant cover at and near the vicinity of the ice edge because of the recurring ice breaking action of sea and swell. Floes or areas of first-year ice (of like age and thickness) are not uncommon and are usually well covered with pressure ridges and hummocks. Other ice types of lesser concentration include small areas of young ice, nilas, and newer types.

Climatic conditions in this area further increase the complexity of sea ice and snow properties throughout the ice season. A wide, fluctuating range of air temperatures along with intermittent periods of rain and snow may significantly affect the radar backscatter.

All the above mentioned factors may contribute to a large diversity in the lateral distribution of surface roughness and dielectric properties as well as subsurface properties. The result is a sea ice terrain which presents a complex radar backscattering surface.

III. RESULTS

Typical ice conditions in the Labrador Sea are not representative of typical ice conditions in most arctic regions. Consequently, so-called radar imagery interpretational keys that are useful for the majority of sea ice conditions may not apply to the Labrador Sea radar imagery, because of the extremely high density surface roughness of so much of the ice that is present here. This high surface roughness is due to an incessant interaction of many small ice forms developed by frequent wave and swell incidence on the ice fields. Parameters which may be influencing the radar returns can include surface roughness in wavelength units, dielectric and conducting properties, physical resonances, surface slopes, and sub-surface effects where significant penetration has occurred. At present, insufficient knowledge about electromagnetic signals and the sea ice environment precludes a good understanding of many of the image measurements. In some cases, a reasonable (though perhaps incorrect) explanation for radar image measurements can be gained by cross-correlating the radar image with coincident photography. In other cases imaged radar backscatter cannot be easily related to visual observations. Interestingly, at times in some areas of sea ice which appear on the photography to have specular surfaces, very little or no backscatter is received on the X-band radar, but significant returns are received by the L-band radar. It is suggested that L-band radar penetration of the sea ice

has occurred and that backscattering parameters that are significant for the surface have become significant at various subsurfaces.

It quickly became apparent during analysis that gray tones and shapes could not always be used in the usual classical sense for the identification and discrimination of many sea ice conditions. The principal reason for this, as mentioned, was the surface roughness characteristics of the Labrador Sea ice. Moreover, differences were noted between the two frequencies and polarizations used in this experiment. The surface roughness characteristics are believed to be an important factor in contributing to the return signal polarizations. Studies have shown (Ellermier et al, 1966) that the polarization of radar returns may be a function of the orientation of the plane of the target slope angle with respect to the plane of the radar incident angle. The signals will remain parallel polarized if the terrain slopes are parallel to the plane of incidence, but may be cross polarized if the planes of the slopes are normal to the incident plane. Most of the very rough ice breccias in the Labrador Sea present many surface slopes with some randomness both in degree and orientation. Very small or only minor differences are noted between backscattering characteristics of the parallel- and cross-polarized imagery of these areas shown on the X-band and L-band imagery. This observation tends to support the theoretical and empirical observations of the earlier studies.

Wide variations in surface roughness on many of the floes of ice breccia often make their identification as discrete forms very difficult or impossible on the X-band imagery. These floes give widely varying radar returns which may be similar to those returns from the surrounding unconsolidated ice, thus preventing their discrimination. However, on the L-band radar the floes of rough ice breccia display a darker, more uniform gray tone and texture than on the X-band radar imagery. Thus they stand out as distinct forms against the surrounding unconsolidated ice matrix of small forms which provide a high contrasting background return on the L-band imagery.

Areas of first-year ice (of the same age), even though they may have an intricate network of ridges and hummocks, do not provide the overall high returns which are characteristic of the rough surfaced ice breccias. Individual ridges often can be identified on this first-year ice because the background return is generally lower than that from the ridges. Other younger areas of ice which have not experienced a great deal of deformation usually provide low return surfaces. Discrimination of these areas from smooth first-year ice could present a problem, but other clues such as rafting, the nature of fracture patterns, and sometimes shape will often enable a confident interpretation.

IV. INTERPRETIVE ILLUSTRATIONS

All the radar imagery shown in the following figures was collected using a 30° antenna depression angle. Near range of this imagery was at nadir and appears at the bottom of each radar image shown. The images are slant range presentations, consequently, the imagery has a range scale compression proportional to the cosine of the target depression angle. Each radar illustration shows both X-band and L-band parallel (horizontal - horizontal) and cross (horizontal - vertical) polarizations. The X-band radar had an approximate 3 cm wavelength, the L-band radar was centered at a wavelength of about 24 cm. Radar image strips have a range scale of 5 nautical miles. However, some of the imagery has been slightly cropped in null areas at near and far range, reducing the range display to something slightly less than 5 nautical miles. The 70 mm radar strips shown in Figures 1 and 2 are at original scale. Radar images shown in the remaining illustrations have been enlarged three times from their original 70 mm size. The enlarged 70 mm photography

was collected simultaneously with the SAR data looking from the right side of the ERIM C-46 aircraft. The camera look angle was not aligned normal to the flight track, but rather was looking somewhat aft of the beam direction. This will be evident when comparing the radar imagery and photography.

The radar imagery quality is generally adequate, however nulls in the antenna pattern tend to obscure some areas. This is most true with the L-band imagery, particularly with the parallel-polarized imagery.

Figure 1 shows sections of X- and L-band parallel and cross polarized imagery taken simultaneously on 13 March 1977 over the area extending seaward from the fast ice off Hopedale Run. The X-band parallel and cross polarized imagery display similar patterns, but there are significant differences in the intensity of radar return or image gray tone of some areas and features on the two image strips. For example, there are two large areas (labeled consolidated rough FY ice) which appear much darker toned on the X-band cross polarized imagery than on the X-band parallel polarized imagery. These areas represent well deformed areas of first-year ice of the same age, but do not possess the very high density surface roughness which is present on the surrounding ice breccias. Roughness necessary for depolarization of the radar signal are not as dominant on the deformed first-year ice (same age) as on the surrounding very rough ice breccias.

The parallel and cross polarized L-band imagery in Figure 1 appear very similar to each other in both pattern and relative image gray tones. On both L-band channels in the areas denoted as consolidated rough FY ice there appear to be significant returns from areas which provide only low returns on the shorter wavelength X-band channels. This anomalous effect suggests that the ice has been penetrated by the L-band radar and that a backscattering subsurface exists, one which possesses properties necessary for signal depolarization. When looking at the major differences in the X- and L-band imagery patterns and gray tones on the image strips in Figure 1, it is evident that radar frequency and polarization considerations can be important in the classification of sea ice parameters. For example, some of the floes of ice breccia which are comprised of a mixture of small areas of deformed and undeformed ice appear as mottled or splotchy textured images on the X-band imagery and cannot be distinguished from the very close packed or compacted mixture of brash and fragments of breccia lying between them. However, on the L-band imagery the floes or consolidated ice breccia are displayed in a more homogeneous, darker toned image than the surrounding matrix of brash and unconsolidated breccia which provides a higher return, thus enabling floe distinction. But, if the ice breccias have a more continuous uniform surface roughness, then the X-band image portrayal has a more homogeneous gray tone and it appears similar to the L-band image of the same feature. It is apparent here that on the L-band imagery both surface conditions appear in a rather homogeneous gray tone. Thus, the L-band radar enables a better interpretation of the distribution of the ice breccia floes, but the X-band radar is a better indicator of surface structure and roughness distribution.

In Figure 2 the ice image patterns, textures, and gray tones are very similar on all four radar channels. As was discussed with Figure 1, this indicates that the area shown is comprised primarily of consolidated rough ice breccia having a rather continuous uniform surface roughness. The major difference between the X- and L-band images in this area is the higher L-band radar return from the very close brash and fragments of ice breccia lying between the rough surfaced floes. Because of this distinction the L-band channels, particularly the parallel polarized L-band imagery, enable an easier interpretation of floe distribution as has been mentioned. Radar backscattering differences between the parallel and cross polarized images of each frequency are relatively minor suggesting the presence of effective depolarizing properties.

Areas of no return open water and/or thin ice cover scattered throughout the scene are in evidence on all four channels. In some cases evidence of a thin ice cover can be seen in low radar returns, but a lack of return does not necessarily mean the area is ice free.

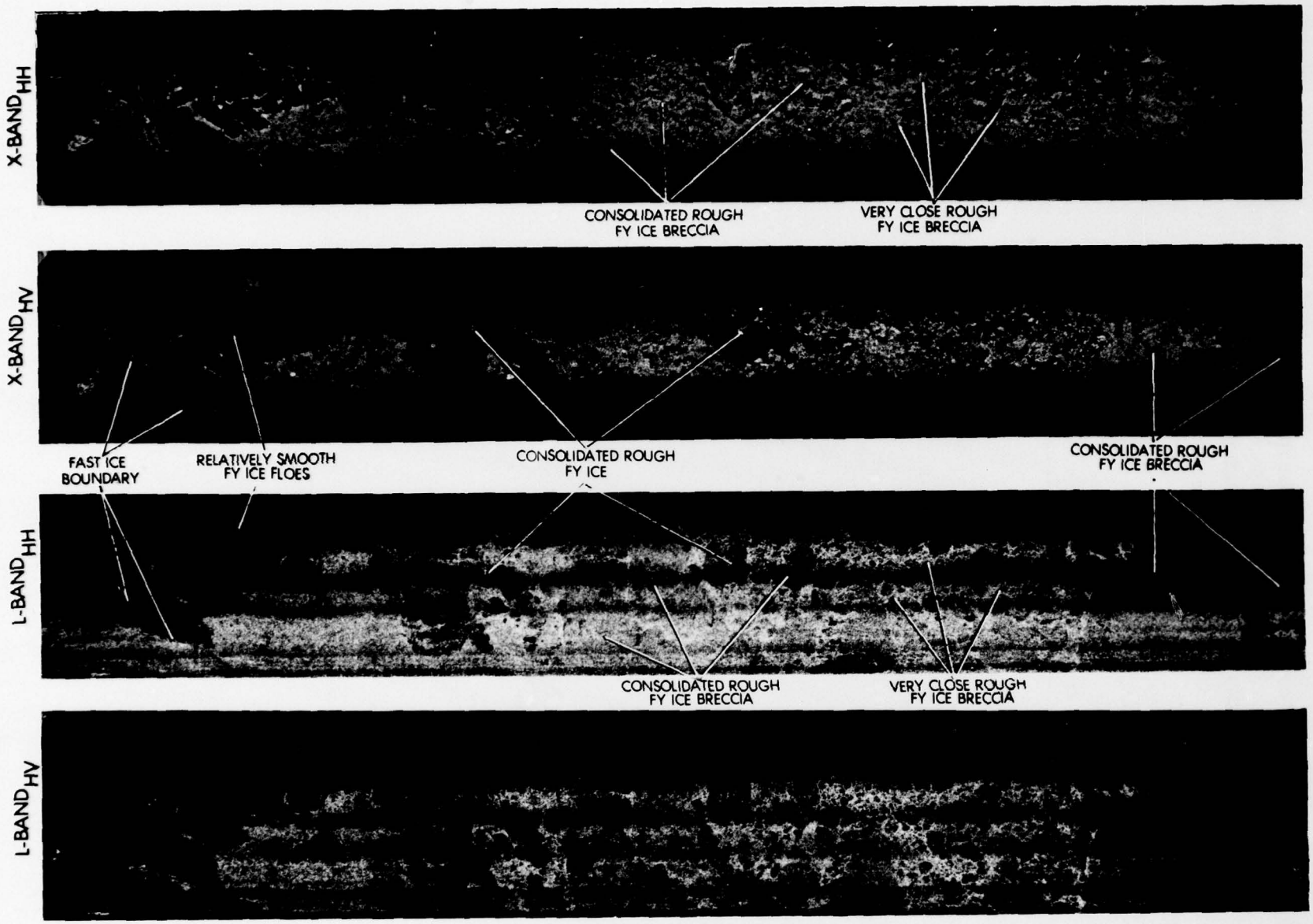

Figure 1. Simultaneous radar images of sea ice off Hopedale Run, Labrador taken by ERIM radar system, 13 March 1977.

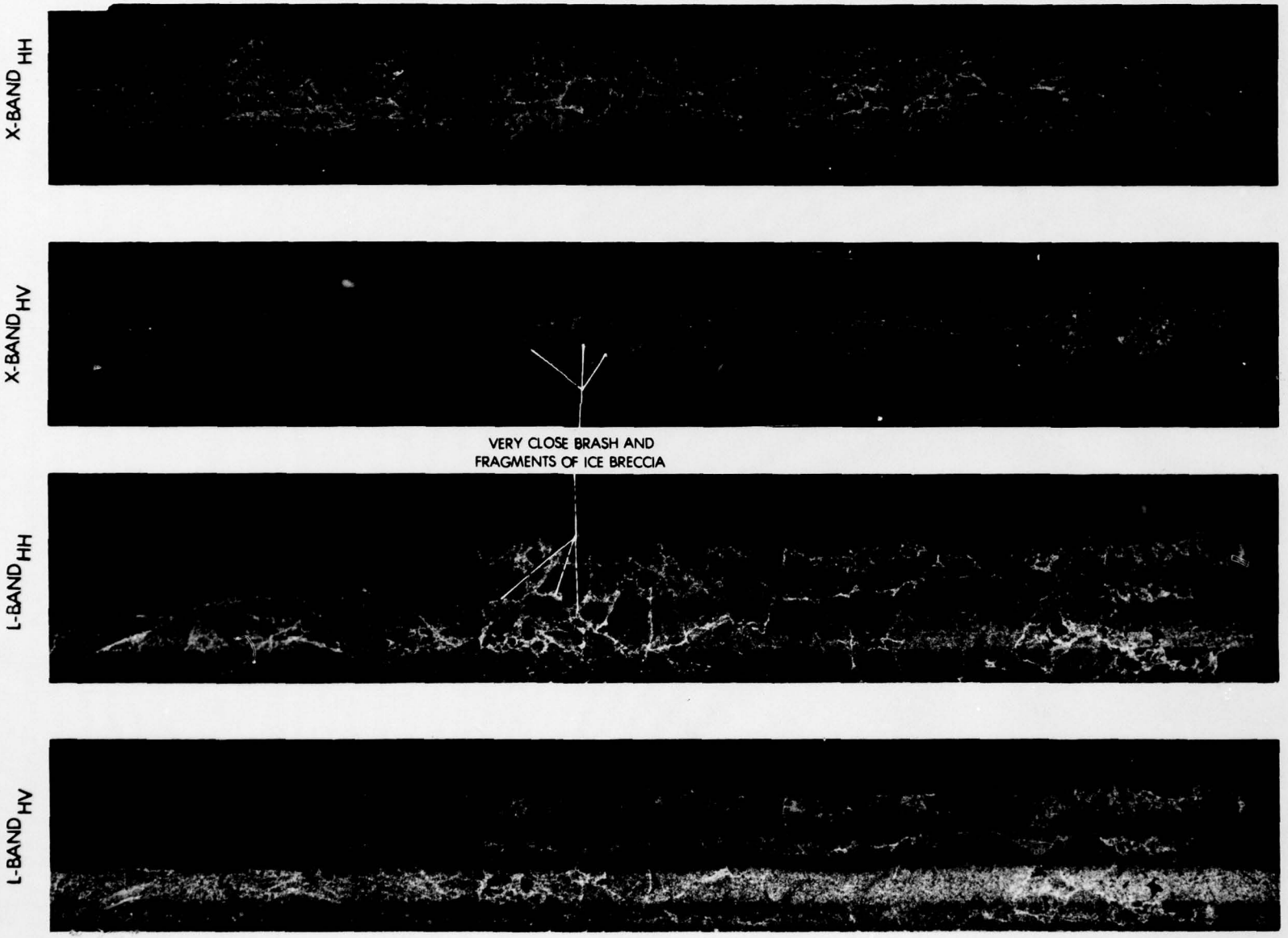

Figure 2. Simultaneous radar images of sea ice off Hopedale Run, Labrador taken by ERIM radar system, 13 March 1977.

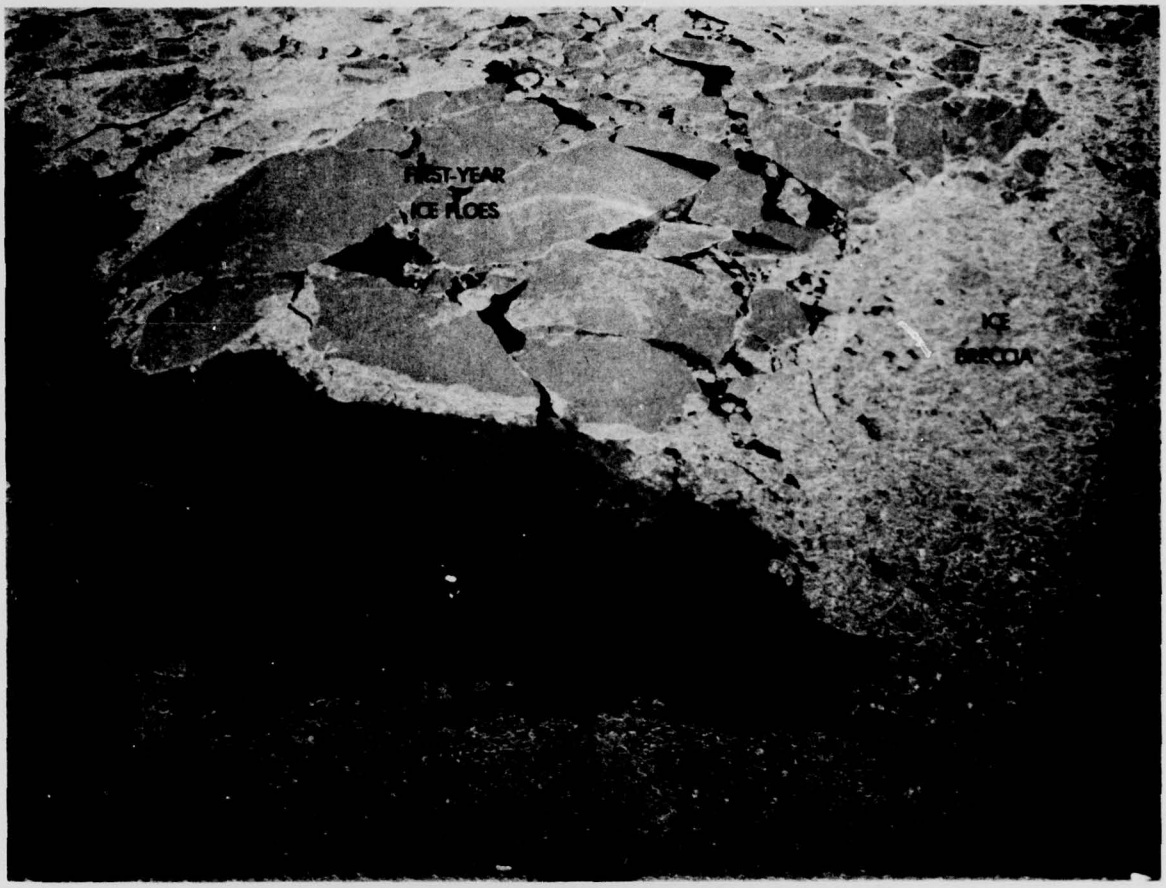

Figure 3. Oblique aerial photograph.

In Figures 3 and 4 the coincident visual and SAR imagery show an area of close pack ice lying immediately seaward of the fast ice off Hopedale Run. The fast ice, which provides a rather high homogenous backscatter on all four radar channels, is comprised of a very rough consolidated mixture of well rounded ice cakes with well deformed borders held together in a frozen matrix of brash. The boundary between the fast ice and nilas is clearly delineated on the L-band channels because of the contrasting low return from the nilas. This sharp demarcation is not so clear on the X-band channels because unusually high radar returns were received from the nilas. The reason for the high return on the X-band imagery from the apparently smooth surfaced nilas is not clear. The rafting in the nilas is best depicted by the X-band parallel polarized and the L-band cross polarized imagery. However, it is almost completely obscure in the X-band cross polarized imagery. Fractures in the nilas are clearly discerned on the X-band imagery, but obscure on the L-band imagery.

The low return floes of relatively smooth first-year ice stand out sharply, clustered in the middle of the scene and scattered throughout the high return rough ice breccias at the top of the scene. Their angular shapes and relatively undeformed nature indicate that they have not been a part of the drifting ice pack for very long. The nilas interspersed among the cluster of first-year ice floes provides a radar backscatter similar to the nilas at the fast ice boundary. On the X-band imagery the high return nilas is contrasted well with the first-year ice floes, but appears very similar to the rough ice breccia bordering some of these floes. On the L-band imagery the nilas appears similar to the first-year ice in gray tone and shape character. In both cases interpretations could be ambiguous.

X-BAND $_{HH}$

X-BAND $_{HV}$

L-BAND $_{HH}$

L-BAND $_{HV}$

Figure 4. Simultaneous radar images from ERIM radar system.

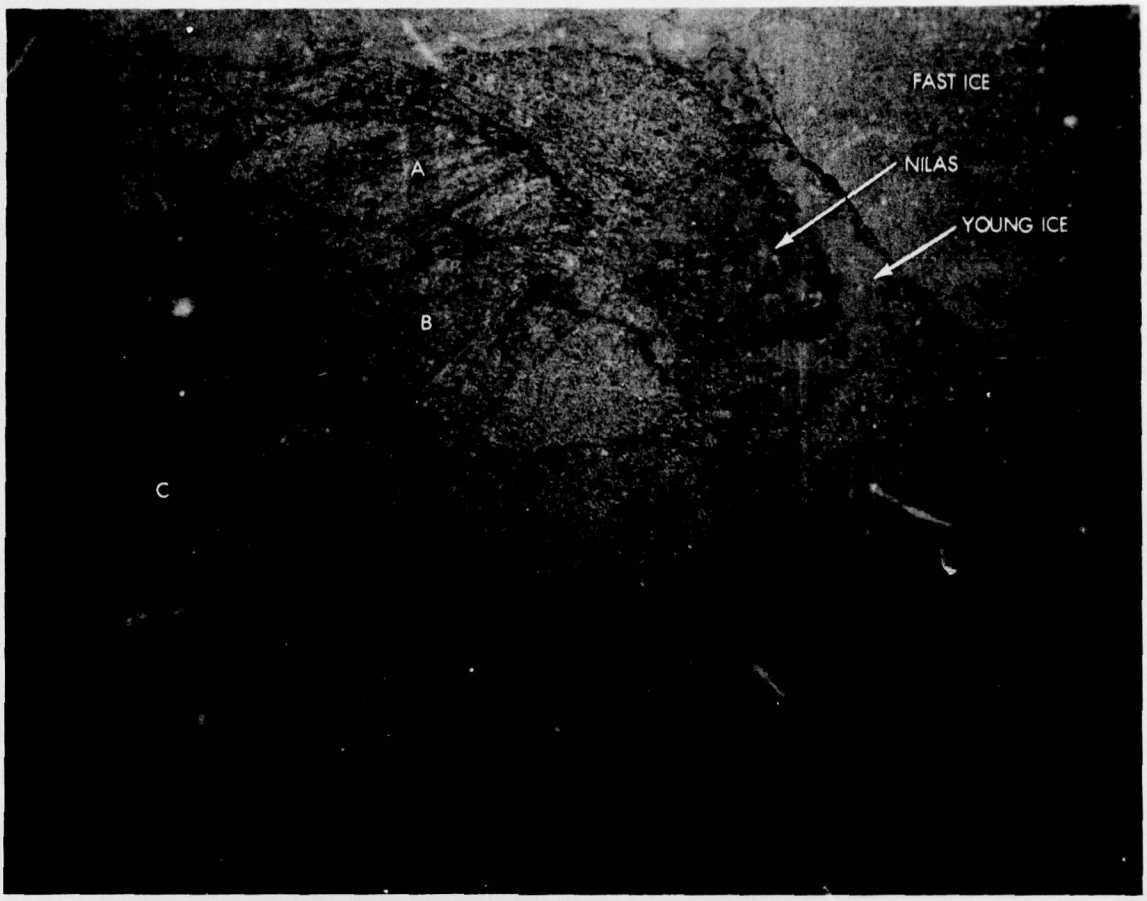

Figure 5. Oblique aerial photograph.

Coincident visual and SAR imagery in Figures 5 and 6 illustrate another area of sea ice located adjacent to the fast ice boundary off Hopedale Run. The area is comprised mainly of consolidated rough ice breccia in a rough matrix of brash and other small forms. The extreme roughness of the surface produces a very high radar backscatter on all four radar channels. However, there are major variations between the X and L-band images even though the parallel and cross polarized images for each of these frequencies are very similar. On the visual image it can be seen that some of the ice breccias such as at A, B and C, contain many small forms which appear to have relatively smooth surfaces. This difference is detected by the X-band radar which shows lower returns from these areas than from the much rougher background. This difference in surface roughness is not very apparent on the L-band imagery where fairly strong returns are being received from the smoother areas as well as the rougher background. We would expect to receive less backscatter of the longer wavelength L-band signal from this surface. Subsurface returns may well account for some of the high backscatter.

The nilas and young ice next to the fast ice boundary provide a fairly high return of the X-band radar as it did in Figure 4. The area of nilas appears to provide a higher return than the thicker young ice on the cross polarized channels. The presence of these radar returns from areas of sea ice which appear to have specular surfaces suggests some penetration and subsurface reflection. Sea ice crystal structure, size, and orientation may be important factors which contribute to subsurface reflection and polarization effects in the early stages of ice development.

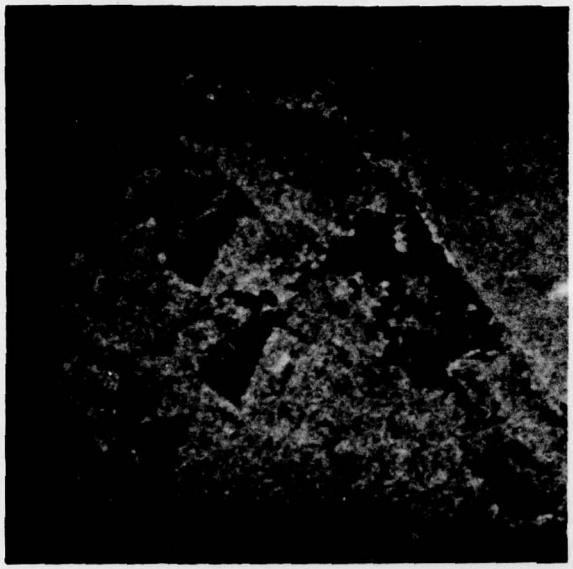

A X-BAND$_{HH}$

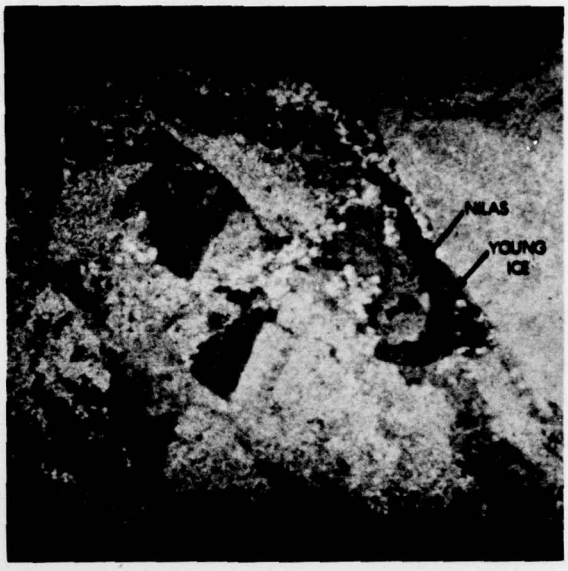

B X-BAND$_{HV}$

C L-BAND$_{HH}$

D L-BAND$_{HV}$

Figure 6. Simultaneous radar images from ERIM radar system.

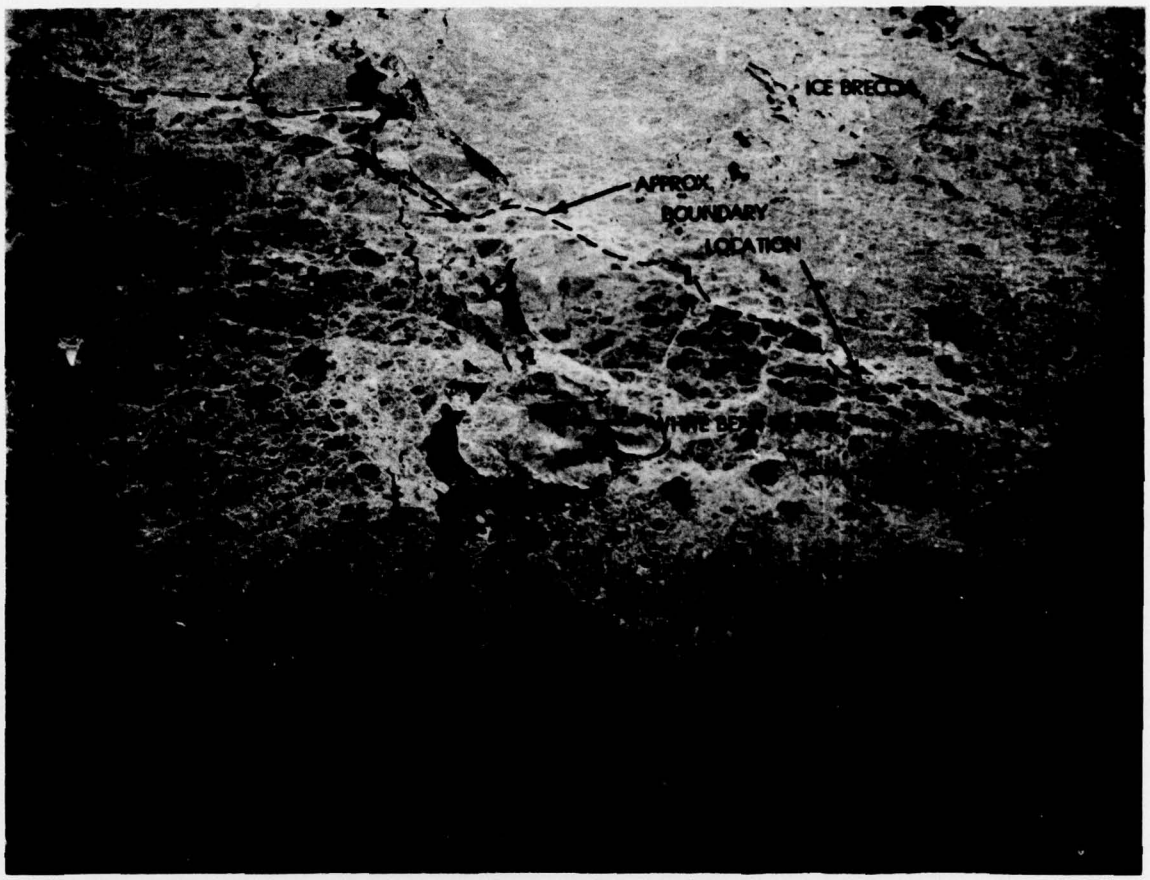

Figure 7. Oblique aerial photograph.

The upper right portion of the coincident imagery in Figures 7 and 8 is covered with a very rough ice breccia in a very close pack of consolidated state. The lower left portion of the imagery is comprised of a well deformed area of first-year ice of like age. A tongue of very rough ice breccia extends into the first-year ice in the vicinity of White Bear Island. Basically different ice surface roughness conditions common to the Labrador Sea are represented here. On the X-band imagery the splotchy textured gray tones in the upper area of the ice breccia indicate the presence of small smooth surfaced areas of ice and/or water interspersed among the rougher ice breccias. The more continuous gray tone on the X-band imagery of the tongue of breccia near White Bear Island indicates a more continuous surface roughness. The L-band radar does not discriminate the surface roughness variations within the ice breccias, and provides a uniformed textured gray tone display for both these areas. In addition, the surface roughness characteristics of the first-year ice in the lower left portion of the scene are better displayed by the X-band radar. Again the L-band radar seems to exhibit more backscatter than can be explained by surface roughness parameters indicating subsurface reflections. The pattern of ridges in the first-year ice is better displayed by the X-band radar channels largely because background noise tends to obscure some of these on the L-band images. The boundary between the two major areas of ice shown in this scene is well delineated on the X-band imagery, particularly the cross polarized X-band imagery. This boundary cannot be identified on the L-band imagery.

The large fractures and polynyas in this area are discernible and can be identified primarily because of their low returns and shapes.

X-BAND $_{HH}$

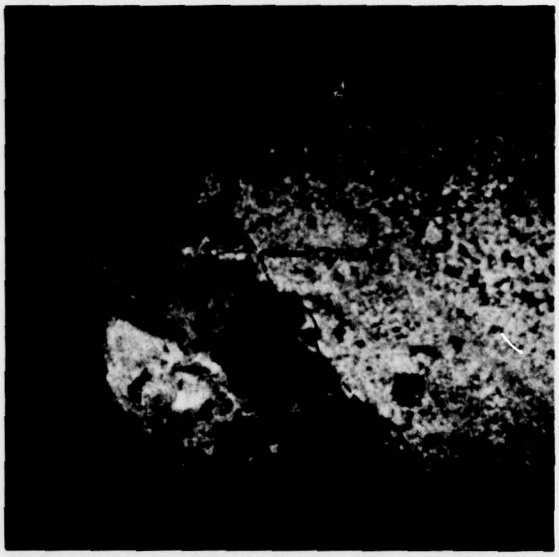

X-BAND $_{HV}$

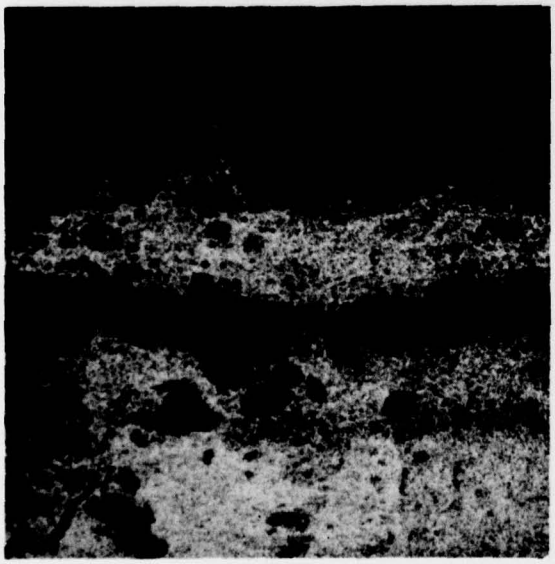

L-BAND $_{HH}$

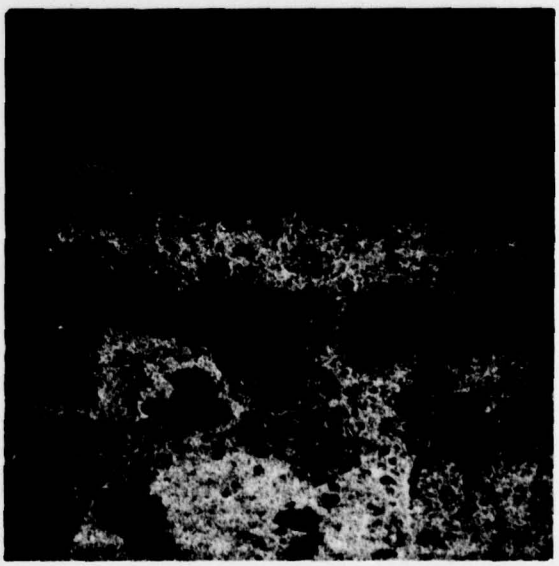

L-BAND $_{HV}$

Figure 8. Simultaneous radar images from ERIM radar system.

Figure 9. Oblique aerial photograph.

Classification of four basically different ice surface conditions in Figures 9 and 10 is made most possible by the distinctive differences in image gray tones and patterns displayed by the X-band cross polarized imagery complemented with information from the other imagery. The generally low radar returns from Area A, with the exception of the ridges, indicates that this is a deformed area of first-year ice of like age. The variegated gray tones and very spotchy image texture of Area B, best shown on the X-band cross polarized imagery, represent a conglomeration of many small ice forms, some possessing relatively smooth surfaces, some possessing extremely rough surfaces. The very high returns have been ascribed in earlier discussion to the strong depolarizing effect of rough surfaces containing multiple reflectors with random slope distributions. In Area C, the rather uniform radar return is attributed to a dense distribution of very close packed small forms having relatively smooth surfaces, but bordered by ridges and hummocks. Much of the radar return from this area could be from freeboard areas as well as from the ridges and hummocks. Area C does not depolarize the X-band signal so effectively as did Area B. The rather high, homogeneous gray tone on all channels depicting the ice in Area D indicates the presence of floes of ice breccia having a rather uniform and dense distribution of radar scatterers. As mentioned, the four areas are best discriminated by the X-band cross polarized imagery. This is primarily due to the strong depolarizing effect of the rough surfaced small forms in Area B and the ineffective depolarizing conditions in Area C. The four areas can be discriminated on the X-band parallel polarized imagery, but not as distinctively. On the L-band imagery there is no strong distinction between Areas B and C and the boundary between C and D is rather obscure.

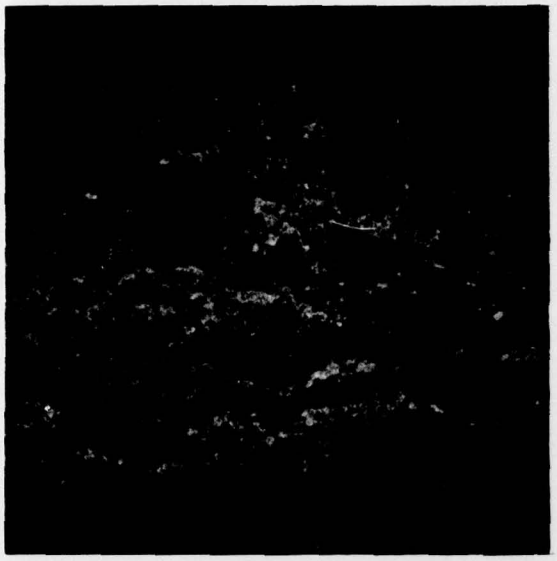

X-BAND HH

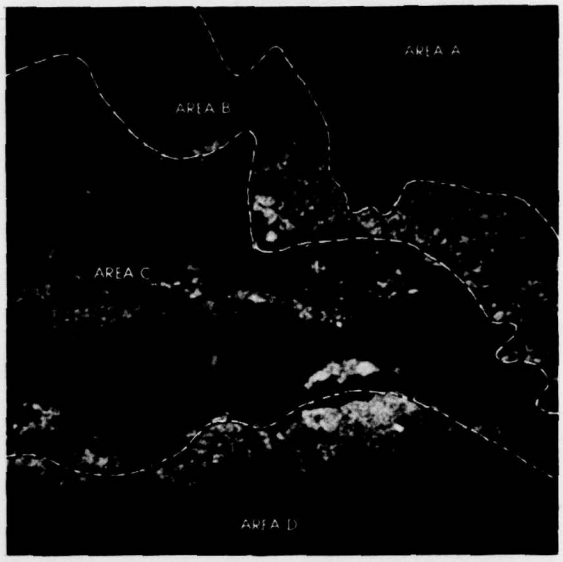

X-BAND HV

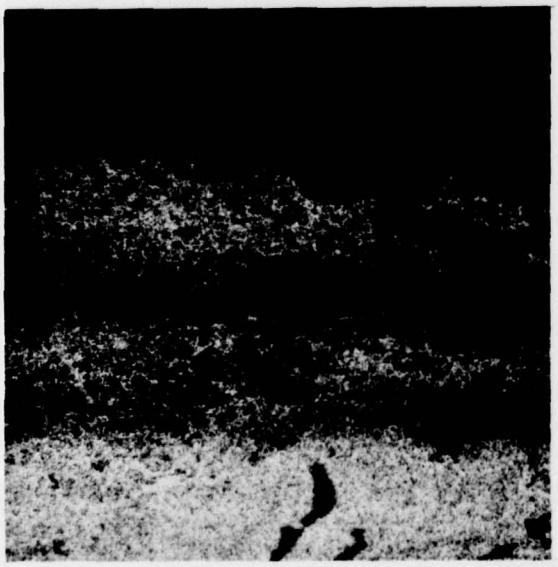

L-BAND HH

L-BAND HV

Figure 10. Simultaneous radar images from ERIM radar system.

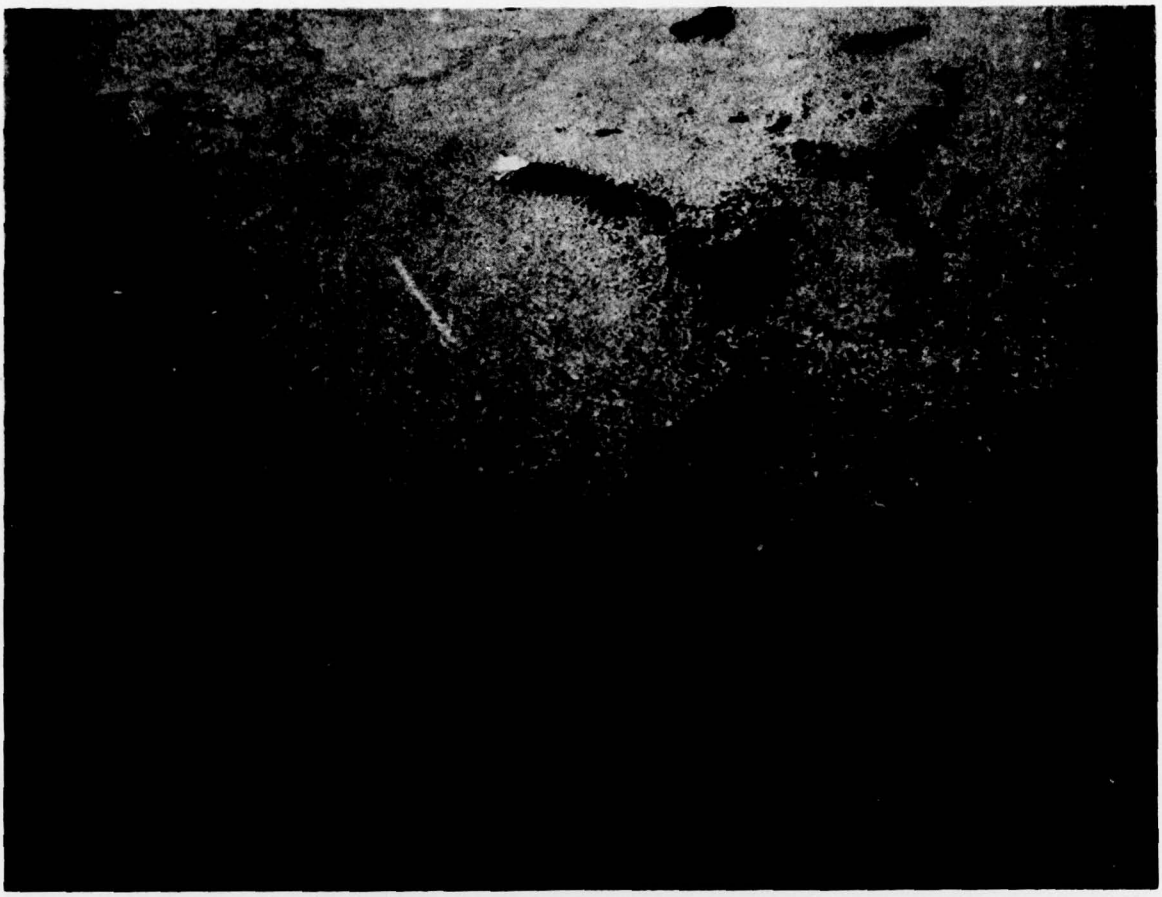

Figure 11. Oblique aerial photograph.

Figures 11 and 12 show coincident visual and radar imagery of an area near the ice edge which has been penetrated by ocean swell. The presence of the swell is apparent on the radar imagery, but is imperceptible on the visual image. It is apparent that the swell action has effectively reduced the ice field to many small floes and cakes. The larger, rougher, and apparently thicker floes concentrated in the central section of the scene have effectively depolarized the radar signals. This area stands out in sharp contrast to its background on the X-band cross polarized imagery. It is postulated that the floes in this area were derived from a larger floe or floes of rough ice breccia which drifted away from the main ice pack and subsequently were effectively broken into many uniform sized fragments by the action of swell. It is interesting to note that these apparent thicker, rougher floes have a somewhat larger average diameter than the surrounding younger floes which appear to be thinner. This suggests that there may be some correlation between the diameter of swell broken ice fragments and ice thickness as well as with the wavelength of the swell.

The iceberg shown in Figures 11 and 12 gives a good radar return on all four radar channels, but its shape and radar shadow appear much sharper on the X-band imagery. One reason for this is the lower background return on the L-band imagery reducing signal contrast, but the rather fuzzy and slightly different shape of the L-band iceberg image could be related to internal reflections.

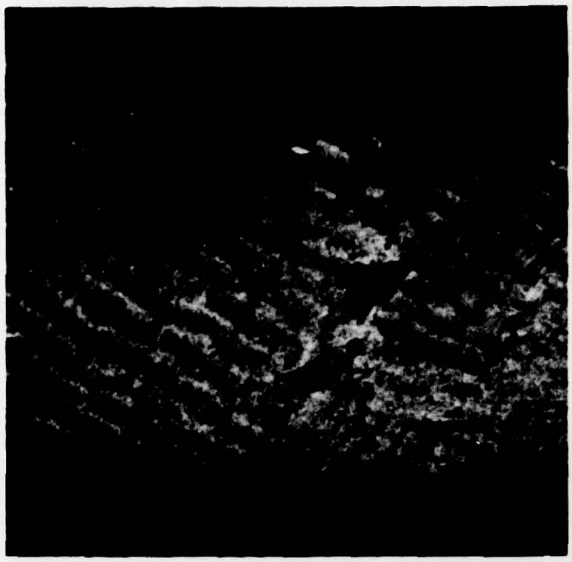

X-BAND $_{HH}$

X-BAND $_{HV}$

L-BAND $_{HH}$

L-BAND $_{HV}$

Figure 12. Simultaneous radar images from ERIM radar system.

V. CONCLUSIONS

The predominance of ice breccias, the high density surface roughness, and the fragmented nature of the ice cover imaged during this SAR experiment was strongly related to the continual incidence of sea and swell on the ice fields of the Labrador Sea. These complex conditions are considered characteristic in the fringe areas of the marginal ice zones so they could be anticipated in fringe areas of the Greenland Sea, the Bering Sea and other areas where the ice edge is exposed to the open ocean. Because the ice and weather conditions of these areas are typically different from most ice covered areas deeper within the ice pack, many of the ice properties which affect the radar backscatter could also be different. For this reason interpretational clues and postulations which have been presented above are not necessarily applicable to all sea ice covered areas.

More ice information can be extracted using simultaneous images of both radar frequencies and polarizations. This was particularly true in the very rough surface areas comprised of consolidated and unconsolidated mixtures of various ages of ice. The L-band imagery provides a better presentation of floe distribution whereas the X-band imagery more accurately provides a display of surface roughness distribution. Determination of surface roughness variations could be accomplished through comparison of the X-band parallel and cross polarized imagery. The variable depolarizing effects caused by variations in surface roughness could enable a better surface roughness description, but ground truth efforts are needed to document the surface variations. Very little difference was noted between the parallel and cross polarization L-band channels regardless of the ice conditions.

It is notable that in the majority of the imagery examined the general image pattern and degree of backscatter displayed by the two L-band channels were very similar. This indicates that backscatter criteria necessary for the depolarization of the L-band signal are usually present in the ice. With the X-band channels, although the ice image patterns are usually very similar, there are occasional marked differences in the intensity of radar backscatter from some of the smoother areas. In these cases a lower backscatter is usually evident on the X-band cross polarized imagery. This effect agrees with earlier theoretical and empirical observations (Ellermeier, et al., 1966) which have indicated that the polarization of the radar return may be a function of the orientation of the plane of the target slope angle with respect to the plane of the radar incident angle. A reduced number of target slope angles oriented normal to the radar incident plane would reduce the depolarizing effect. In any event, it would seem that if there is a lack of depolarizing features for X-band signals, then there would also be a lack of depolarizing features for the longer wavelength L-band signals if the same backscattering interface was being considered. However, some of the image examples have indicated a good depolarization of the L-band signal when depolarization of the X-band signal seemed rather weak. This suggests that more than one backscattering interface exists. The X-band radar returns seem to correlate well with the visible surface structure, but the L-band radar returns do not always correlate well with the surface roughness (e.g., often good returns are seen from apparently smooth areas). The ERIM sea ice imagery taken in this experiment strongly indicates that at times the backscatter interface for L-band radar is a subsurface structure and that interface is usually conducive to the depolarization of the L-band signal. It is likely at times that both surface and subsurface reflections are being received from the same area of ice.

In addition to the strong indications that subsurface returns were being received by the L-band radar, there was also some suggestion that, at times, subsurface returns were

received by the X-band radar. This was true with some of the apparently smooth surfaced early stages of ice development such as nilas and young ice when fairly strong returns were displayed on both the parallel and cross polarized imagery. It was suggested that sea ice crystal structure, size, and orientation in these early stages of ice development may be important factors contributing to the reflection and polarization effects on radar energy which has penetrated the ice surface.

VI. REFERENCES

Ellermeier, R. D., A. K. Fung, D. S. Simonett, Some Empirical and Theoretical Interpretations of Multiple Polarization Radar Data, CRES Report No. 61-10, University of Kansas, Lawrence, Kansas, 1966.

Ketchum, R. D. Jr., An Evaluation of Side Looking Radar Imagery of Sea Ice Features and Conditions in the Lincoln Sea, Nares Strait, and Baffin Bay, NORDA Technical Note 7, April 1977.

Ketchum, R. D. Jr., S. G. Tooma, Interpretation Analysis of Airborne Multi-Frequency Side Looking Radar Sea Ice Imagery, Journal of Geophysical Research, Vol. 78, No. 3, 1973.

Rawson, R., F. Smith, C. Kiskow, R. Shuchman, R. Larson, Field Data Report, "Investigation of the Characterization of Sea Ice and Icebergs Using the ERIM X-L Band Airborne Synthetic Aperture Radar." Environmental Research Institute of Michigan, July 1977.

Worsfold, R. D., D. Strong, E. Wedler, Project SAR 77 (Preprint), POAC 77, Fourth International Conference on Port and Ocean Engineering Under Arctic Conditions, Memorial University of Newfoundland, Sept. 1977.

UNCLASSIFIED

SECURITY CLASSIFICATION OF THIS PAGE (When Data Entered)

REPORT DOCUMENTATION PAGE

READ INSTRUCTIONS BEFORE COMPLETING FORM

1. REPORT NUMBER: NORDA TECHNICAL NOTE 28

2. GOVT ACCESSION NO.

3. RECIPIENT'S CATALOG NUMBER: NORDA-TN-28

4. TITLE (and Subtitle): An Evaluation of ERIM X-L Band Airborne Synthetic Aperture Radar Imagery of Sea Ice

5. TYPE OF REPORT & PERIOD COVERED: Final

6. PERFORMING ORG. REPORT NUMBER

7. AUTHOR(s): R. D. Ketchum, Jr

8. CONTRACT OR GRANT NUMBER(s): None

9. PERFORMING ORGANIZATION NAME AND ADDRESS: Naval Ocean Research and Development Activity, NSTL Station, MS 39529

10. PROGRAM ELEMENT, PROJECT, TASK AREA & WORK UNIT NUMBERS: 62759N-ZF52-552-001, 330-9332030

11. CONTROLLING OFFICE NAME AND ADDRESS: Same as 9

12. REPORT DATE: July 1978

13. NUMBER OF PAGES: 25

14. MONITORING AGENCY NAME & ADDRESS (if different from Controlling Office): Same as 9

15. SECURITY CLASS. (of this report): Unclassified

15a. DECLASSIFICATION/DOWNGRADING SCHEDULE

16. DISTRIBUTION STATEMENT (of this Report): Distribution unlimited

DISTRIBUTION STATEMENT A
Approved for public release; Distribution Unlimited

17. DISTRIBUTION STATEMENT (of the abstract entered in Block 20, if different from Report): Same as 16

18. SUPPLEMENTARY NOTES

19. KEY WORDS (Continue on reverse side if necessary and identify by block number): Synthetic aperture radar, radar backscatter, radar polarization, sea ice

20. ABSTRACT (Continue on reverse side if necessary and identify by block number)

Results of an evaluation of the ERIM X-L band airborne synthetic aperture radar imagery of sea ice in the Labrador Sea are given. Incident sea and swell and surface winds in this area produce complex and chaotic ice conditions with very rough surfaced ice breccias being the dominant form. It was possible to extract more information concerning the ice conditions when using both radar frequencies and polarizations. Surface roughness differences and distribution were more accurately determined using the X-band radar imagery. Variations in the nature of the surface (continue on reverse)

DD FORM 1 JAN 73 1473 EDITION OF 1 NOV 65 IS OBSOLETE
S/N 0102-LF-014-6601

UNCLASSIFIED
SECURITY CLASSIFICATION OF THIS PAGE (When Data Entered)

392 773

20. Abstract - cont:
roughness are sometimes evident due to their varying polarizing effect on the X-band radar. Floe distribution is better displayed by the L-band radar imagery, but only minor differences were recorded by the two L-band radar polarizations. The analysis shows that the X-band radar is more sensitive to ice surface properties, but that surface penetration and subsurface interfaces may account for much of the L-band radar backscatter. There are some indications of X-band subsurface return and depolarization in some very early stages of ice development. This suggests that sea ice crystal structure, size, and orientation in these early stages of ice development may be important contributors to the backscatter and polarization effects on radar energy which has penetrated the surface.